Colloid Polym Sci (2004) 282: 1105–1110
DOI 10.1007/s00396-003-1043-6

ORIGINAL CONTRIBUTION

Akira Tsuchida
Emiko Takyo
Kazunori Taguchi
Tsuneo Okubo

Kinetic analyses of colloidal crystallization in shear flow

Received: 16 September 2003
Accepted: 7 November 2003
Published online: 29 January 2004

A. Tsuchida · E. Takyo · K. Taguchi
T. Okubo (✉)
Department of Applied Chemistry and Graduate School of Materials Science, Gifu University, Gifu 501-1193, Japan
E-mail: okubotsu@apchem.gifu-u.ac.jp
Fax: +81-58-2932628

Abstract Colloidal crystallization kinetics is studied in the shear flow of a suspension of colloidal silica spheres (110 nm in diameter), using a continuously-circulating type of stopped flow cell system. The crystallization rate from a suspension containing a small amount of nuclei and/or single crystals is high compared with that from a suspension containing no nuclei and/or single crystals. Crystal growth takes place at shear rates smaller than 3.4 s^{-1} and at sphere concentrations higher than a volume fraction of 0.004.

Keywords Colloidal crystals · Crystallization kinetics · Crystal growth rate · Shear rate · Reflection spectra

Introduction

The kinetics of colloidal crystallization has been studied by several researchers up to now for two main types of crystal suspensions: diluted and deionized aqueous suspensions where the colloidal particles are covered with electric double layers (called soft-sphere systems) [1, 2, 3, 4, 5, 6, 7, 8, 9, 10, 11, 12, 13, 14, 15, 16, 17, 18, 19, 20, 21], and concentrated suspensions in refractive index-matched organic solvents (called hard-sphere systems) [22, 23, 24, 25, 26, 27, 28, 29, 30, 31, 32, 33, 34, 35, 36, 37, 38, 39, 40]. This classification into soft- and hard-sphere systems depends largely on the ionic concentration of the suspension; in other words we get ''soft'' crystals in a completely deionized environment, and ''hard'' crystals in the presence of large numbers of ions – a rather large amount of sodium chloride, for example.

Many researchers, including us, clarified that colloidal crystals are formed by Brownian movement of colloidal particles in a closed vessel, and also by the interparticle repulsion leading to minimal dead space [8, 41, 42, 43, 44, 45, 46, 47, 48, 49, 50, 51, 52, 53, 54, 55, 56]. In other words, particles form crystal-like arrangements owing to the Brownian movement of the particles that leads to maximum packing density.

We have studied both nucleation and crystallization processes in exhaustively deionized and highly-diluted aqueous suspensions via dynamic light scattering measurements, from the half-widths in the sharpened reflection peak, and from increases in the reflection peak intensity [8, 10, 11, 12, 13, 14, 15, 16, 17, 18, 19, 20, 21]. Though the crystallization process was surprisingly fast, reflection spectroscopy could follow crystallization rates of the order of milliseconds. Nucleation rates increased drastically as sphere concentration increased. Crystal growth rates also increased substantially as the sphere concentration increased [11, 12], but only in a narrow concentration range. Furthermore, nucleation and crystallization rates were very sensitive to the degree of deionization of the aqueous suspensions. Recently, we further studied the kinetics of colloidal crystallization in a sinusoidal electric field [14], in a wide range of sphere concentrations [15], in the presence of salt [16], in alcoholic organic solvents [13], and in organic solvents such as acetonitrile for silica spheres coated with polymers [20, 21]. Microgravity experiments exploring the kinetics

of colloidal crystallization, performed on an aircraft, have also been made by our group [17, 18, 19]. In the course of these studies, we recognized that the colloidal crystallization rate is also strongly dependent on the shear rate of the suspension.

In this work, colloidal crystallization rates were measured using a continuously-circulating type of stopped flow cell system. The colloidal crystallization rates were measured as a function of shear rate of the circulating suspension before and during crystallization in the continuous flow state. These experiments are called initial and final shear flow analyses, respectively, in this work.

Experimental

Materials

Monodispersed colloidal silica spheres (CS91) were kindly donated by Catalyst & Chemicals Ind. Co. (Tokyo). The diameter (d), standard deviation (δ) from the mean diameter, polydispersity index (δ/d), and specific gravity were 110 nm, 4.5 nm, 0.041, and 2.2, respectively. The values of d and δ were determined by electron microscope (JEM-2000FX, JEOL, Tokyo). The charge density of the spheres was determined to be 0.48 μC/cm^2 for strongly acidic groups by conductometric titration with a Horiba model DS-14 conductivity meter. The sphere sample was purified carefully several times using an ultrafiltration cell (model 202, membrane: Diaflo XM, Amicon, Lexington, KY), and then treated with a mixed bed of cation- and anion-exchange resins (Bio-Rad, AG501-X8 (D), 20–50 mesh) for more than five years. The sample suspensions (volume fractions: $\phi = 0.002$, 0.003, 0.004, 0.005 and 0.006) were in most cases deionized further for 30 min after preparation by circulation in the cell system at the shear rate of 15 s^{-1}. The shear rates for the initial and final analyses were changed from 0 to 34 s^{-1}. The water used for sample suspension was obtained from a Milli-Q water system (Milli-RO Plus and Milli-Q Plus, Millipore, Bedford, Mass). Experiments were made at 25 ± 1.5 °C in an air-conditioned room.

Kinetics experiments for colloidal crystallization

The observation cell system, which was the same as one reported previously for the microgravity experiments [17, 18, 19], consists of a quartz observation cell (40×10×2 mm), a column of cation- and anion-exchange resins (Bio-Rad), and a peristaltic pump (Masterflex 7524-10, IL). The pump circulates the colloidal suspension first to the resin column and then to the observation cell in order to deionize the suspension continuously. It has been already checked, using reflection spectroscopy, that 15 s^{-1} of shear rate almost completely breaks the crystals in the system. A light beam from a halogen lamp (Hayashi LA-150SX, Tokyo) hits the cell wall through a Y-type optical fiber cable, and the reflection spectra are taken on a photonic multichannel analyzer (PMA-50, Hamamatsu Photonics, Hamamatsu).

When the colloidal suspension is passed into the narrow observation cell, the crystals are melted away by the flow shear. In this observation cell, a flow rate of 1.0 ml/s corresponds to a shear rate of 1.7 s^{-1}. After stopping the flow the crystallization starts. The crystal growing process was followed from the growth of the Bragg reflection peaks. In our experimental conditions the suspension in the flow cell (2 mm in path length) was transparent. Therefore, the reflection spectroscopy in our experiments will afford information on the crystal growing processes for the whole depth of the suspension in the cell.

Two kinetic analyses were made in this work. The first analysis was made for the measurements of the dependence of the colloidal crystallization rate on the initial shear rate (q_i). In these measurements, the initial equilibrium state was attained at various initial shear rates ($q_i = 1.7$–34 s^{-1}) in the measurement cell. Then the flow was stopped suddenly and the crystallization coefficient was measured by reflection spectroscopy. The second analysis was performed for measurements of the dependence of the colloidal crystallization rate on the final shear rate (q_f). In these measurements, the initial equilibrium state was fixed at the shear rate of 34 s^{-1}. This shear rate is quite enough to break all of the crystals in the cell. Then, the shear rate decreased to various final continuous shear rates ($q_f = 1.7$–15 s^{-1}) and the crystallization rate coefficient was measured.

Results and discussion

Effective soft-sphere model for colloidal crystallization

According to the effective soft-sphere model, which is a simple but very convenient assumption for the colloidal crystallization, crystal-like ordering of the single component spheres occurs when the effective diameter (d_{eff}) of the spheres containing the Debye-screening length (D_l) is close to or larger than the intersphere distance (l):

$$d_{\mathrm{eff}} = (d + 2 \times D_l) > l, \tag{1}$$

$$D_l = \left(\frac{4\pi e^2 n}{\varepsilon k_B T}\right)^{-1/2}, \tag{2}$$

where d is the sphere diameter, e is the electronic charge, ϵ is the dielectric constant of the solvent, k_B is the Boltzmann constant, and n is the concentration of free-state cations and anions in suspension which is given by $n = n_c + n_s + n_o$, where n_c is the concentration (number of ions per cm^3) of diffusible counterions, n_s is the concentration of foreign salt, and n_o is the concentration of both H^+ and OH^- from the dissociation of water. At $\phi = 0.005$ for the CS91 spheres, for example, d_{eff} was calculated to be 800 nm. Here, the fraction of free-state counterions (β) was assumed to be 0.1. This value of d_{eff} was larger than the intersphere distance (l), 580 nm, calculated assuming the sphere distribution of a simple cubic lattice. That $d_{\mathrm{eff}} > l$ lends strong support to the soft-sphere model.

Kinetic analyses of colloidal crystallization

The induction period (the period before the onset of crystal growth) was too short to be observed for most kinetic measurements in this work, considering the comparatively high sphere concentrations [14]. Therefore, the

classical nucleation rates were also not obtained for this study. For reflection spectroscopy, the size of the colloidal single crystals from homogeneous nucleation, L, is estimated from the intensity of the reflection peak, I [26]:

$$I \propto N_{\mathrm{cryst}} L^3 \propto L^3, \tag{3}$$

where N_{cryst} is the number of single crystals in the reflecting volume, which is directly proportional to the number concentration of crystals in the final stage of the crystallization process (equal to the total number of nuclei formed in the whole course of crystallization). Therefore, the rates of crystallization, v, should be evaluated from the slopes of the plots of the cube root of each peak intensity with time [17]. However, preliminary analyses of these plots gave large uncertainties because the concentrations of the suspension ranged from $\phi = 0.001$ to 0.006 (rather high). We therefore introduced the rate coefficient, k, into this work instead of v. The values of k were obtained as the reciprocal period where the initial linear line in the peak intensities intersects two horizontal lines, giving initial and final times at $t = t_{\mathrm{i}}$ and t_{f}, respectively; in other words:

$$k = \frac{1}{t_{\mathrm{f}} - t_{\mathrm{i}}}. \tag{4}$$

The values of t_{i}, which correspond to crystallization induction times, were very close to zero in this work, as mentioned above.

Crystallization rates after stopping the flow under shear flow

Typical reflection spectra taken during the crystallization of CS91 spheres at $\phi = 0.005$ are shown in Fig. 1. The colloidal suspension was initially circulated at a shear rate of $q_{\mathrm{i}} = 34\ \mathrm{s}^{-1}$ for more than 3 min, and the quasi-equilibrium state was attained between the crystallization and melting of the sample in the observation cell. The suspension was then stopped suddenly at $t = 0$, and further crystal growth processes started. Spectra were obtained from $t = 0$ to 19.4 s after stopping the pump. A short time after stopping the flow, we noted the appearance of a broad peak in the higher wavelength region at around 635 nm. Over time, the peak intensity increased with a sharpened peak profile, and the peak wavelengths decreased to around 625 nm. This shift in the peak wavelength is explained by the fact that the metastable and expanded crystal structures are formed first and then the crystals become more stable and dense [16, 17, 18, 19]. The peak wavelength observed is reasonable because the secondary Bragg peak wavelength calculated from the sphere concentration is 633 nm for the simple cubic lattice. The Bragg peaks in Fig. 1 are assigned to face-centered cubic (fcc) lattices because another peak from body-centered cubic (bcc) lattices appeared at lower wavelengths for suspensions of much lower concentration [17]. In the present work, all of the kinetic analyses were made for reflection peaks from fcc lattices.

A typical example of the time dependence of the peak intensities is shown in Fig. 2. As is clear from the figure, crystal growth was almost complete by ~5 s after stopping the flow.

Figure 3 shows the rate coefficient k_{i} for the colloidal crystallization, plotted against q_{i} for the sphere concentration from 0.002 to 0.006. Here, the subscript "i" indicates the initial state suspension. The values of k_{i} are clearly dependent on ϕ and q_{i}. In the concentration range from $\phi = 0.003$ to 0.006, k_{i} decreases as q_{I} increases. The dependency of k_{i} on q_{i} is correlated directly to the rigidity of the colloidal crystal formed in the final state. Furthermore, the partial destruction of the nuclei and/or crystals occurs in the shear flow. Reflection spectroscopy detected the flowing crystals when the suspension was circulated with small q_{i}. At small q_{i},

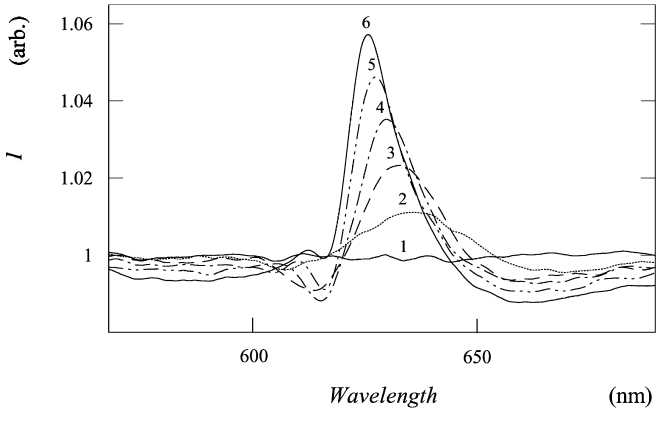

Fig. 1 Reflection spectra for colloidal crystals of CS91 spheres at 25 °C. $\phi = 0.005$; $q_{\mathrm{i}} = 34\ \mathrm{s}^{-1}$; $q_{\mathrm{f}} = 0\ \mathrm{s}^{-1}$. Curve 1: 0 s; 2: 0.7 s; 3:1.3 s; 4:2.1 s; 5:4.4 s; 6:19.4 s after stopping the flow

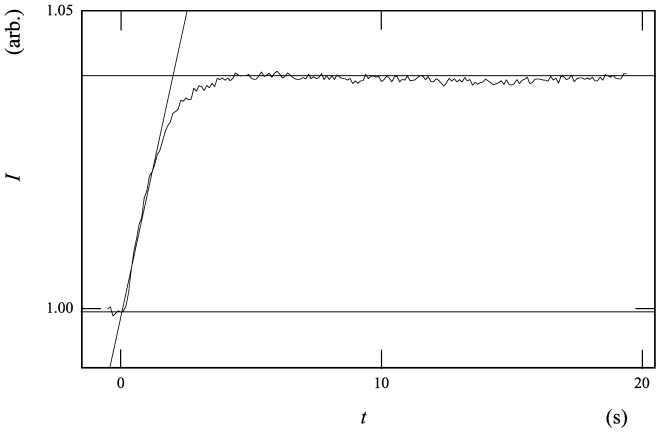

Fig. 2 Reflection peak intensities during the colloidal crystallization of CS91 spheres at 25 °C. $\phi = 0.005$; $q_{\mathrm{i}} = 25\ \mathrm{s}^{-1}$; $q_{\mathrm{f}} = 0\ \mathrm{s}^{-1}$

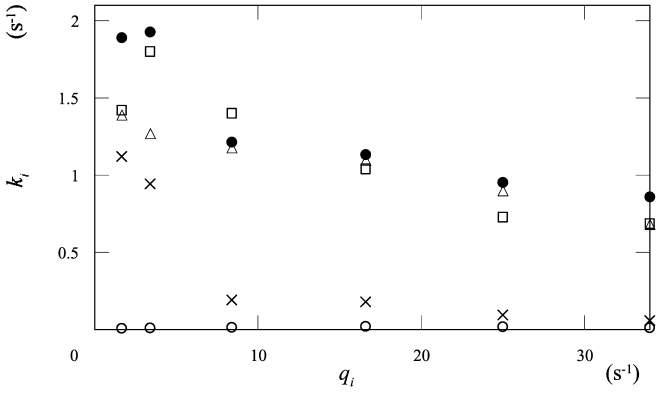

Fig. 3 Rate coefficients (k_i) as a function of initial shear rate (q_i); CS91 spheres at 25 °C; $q_f = 0$ s^{-1}; unfilled circles: $\phi = 0.002$; ×: $\phi = 0.003$; triangles: $\phi = 0.004$; squares: $\phi = 0.005$; filled circles: $\phi = 0.006$

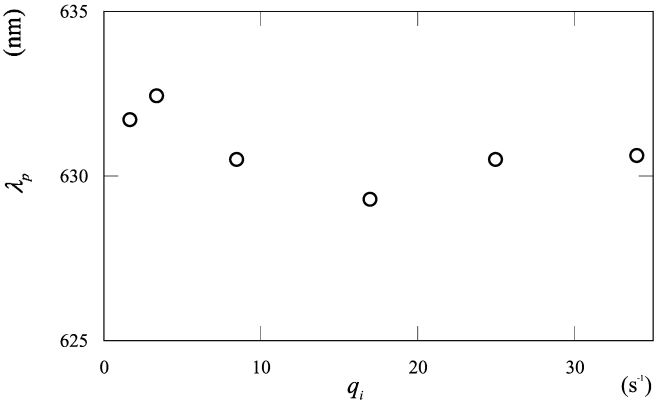

Fig. 4 Reflection peak wavelengths (λ_p) at 19.4 s after stopping the flow, as a function of initial shear rate (q_i). CS91 spheres at 25 °C; $q_f = 0$ s^{-1}; $\phi = 0.005$

especially for $q_i \leq 3.4$ s^{-1}, the crystals and/or nuclei in the suspension will not break up thoroughly, and it is highly plausible that the crystallization is enhanced in the flowing suspension. This means that the crystal growth rate from pre-existing crystals and/or nuclei is higher than that from completely liquid suspension. It should be mentioned that the nucleation time is short enough (less than 20 ms from the resolution of the time-resolved reflection spectra) in the present experimental condition as described above. At $\phi = 0.002$, k_i was independent of q_i, although the values were small (of the order of 10^{-2} s^{-1}). At low sphere concentrations neither crystals nor nuclei must form in the shear flow, because the rigidity of the crystals is very small.

According to classical crystal growth theory [17, 57, 58], the crystal growth rate v is given by:

$$v = v_\infty - v_\infty \frac{\phi_c}{\phi}, \tag{5}$$

where v_∞, ϕ_c and ϕ are the maximum crystallization rate, the critical sphere concentration of melting (in volume fraction), and the sphere concentration, respectively. Therefore, v is expected to increase proportionally with increasing $1/\phi$. This linear relationship between v and $1/\phi$ is obtained when rather large experimental errors in the k_i values are taken into account.

Figure 4 shows the reflection peak wavelength observed at $t = 19.4$ s after stopping the flow, as a function of q_i. Clearly, λ_p was independent of q_i to within an accuracy of 0.5%. This means that the crystals formed in the final step are the same irrespective of q_i.

Crystallization rates when the final stage of the suspension during crystallization is in shear flow

Figure 5 shows a typical example of the reflection peak intensities measured during the course of colloidal crystallization, with initial and final suspension flows at 34 s^{-1} and 3.4 s^{-1}, respectively. In this figure, the suspension was initially circulated at the shear rate of 34 s^{-1} for more than three minutes. Then the flow rate was dropped immediately to $q_f = 3.4$ s^{-1}. After dropping the shear rate at $t = 0$, the intensity of the Bragg peak increased sharply. In the figure, a large number of pulses can be observed. The frequency of the pulses coincided with that of mechanical rotation of the peristaltic pump. Therefore, the remaining pulsating flow of the suspension may cause the crystal growth and melting process periodically.

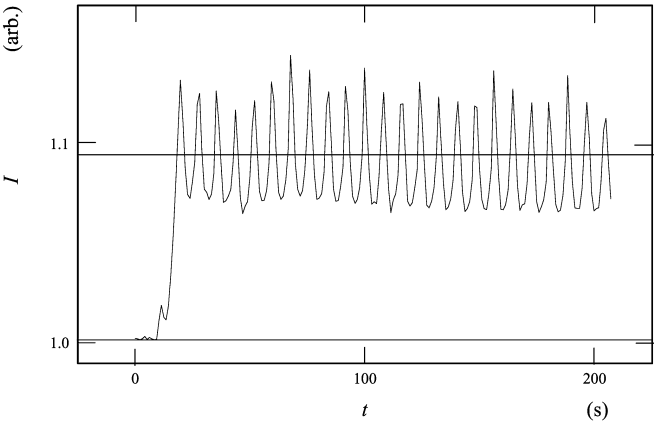

Fig. 5 Reflection peak intensities during colloidal crystallization of CS91 spheres at 25 °C. $\phi = 0.006$; $q_i = 34$ s^{-1}; $q_f = 3.4$ s^{-1}

Figure 6 shows the rate coefficient k_f as a function of q_f for a sphere concentration of 0.003 to 0.006 (volume fraction). Measurements were also made for $\phi = 0.002$ suspension in this work. However, no crystals were formed. Crystallization did not occur at high q_f values either; for example at > 5.1 s^{-1} for $\phi = 0.003$, > 6.8 s^{-1} for $\phi = 0.004$ and > 10.2 s^{-1} for $\phi = 0.005$. At $\phi = 0.003$, crystals were formed, but the Bragg peaks were very faint.

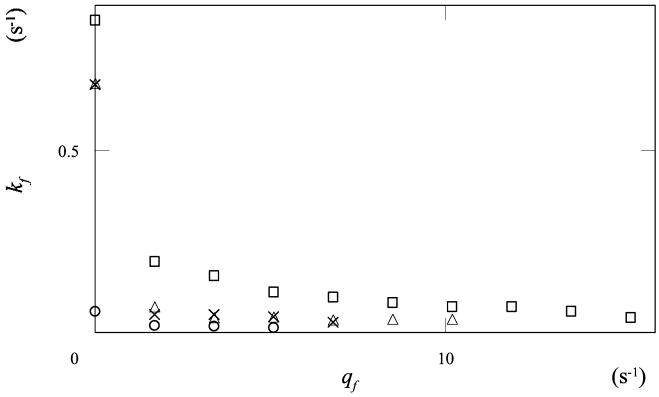

Fig. 6 Rate coefficients (k_f) as a function of final shear rate (q_f), CS91 spheres at 25 °C; $q_i = 34\ s^{-1}$; unfilled circles: $\phi = 0.002$; ×: $\phi = 0.003$; triangles: $\phi = 0.004$; squares: $\phi = 0.005$; filled circles: $\phi = 0.006$

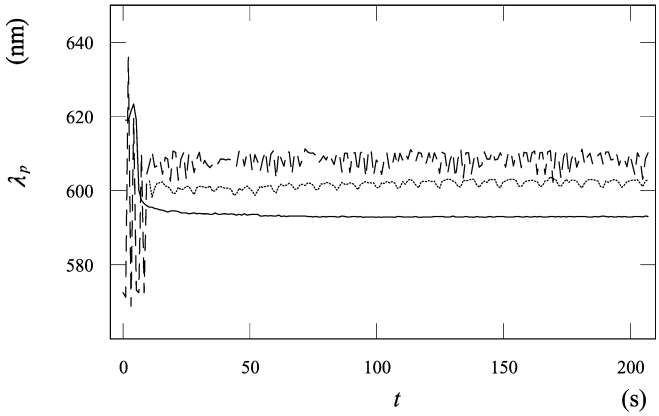

Fig. 7 Time dependence of the reflection peak wavelength during the colloidal crystallization of CS91 spheres at 25 °C. $\phi = 0.006$; $q_i = 34\ s^{-1}$; $q_f = 0\ s^{-1}$ (solid curve); $q_f = 3.4\ s^{-1}$ (dotted curve); $q_f = 6.3\ s^{-1}$ (broken curve)

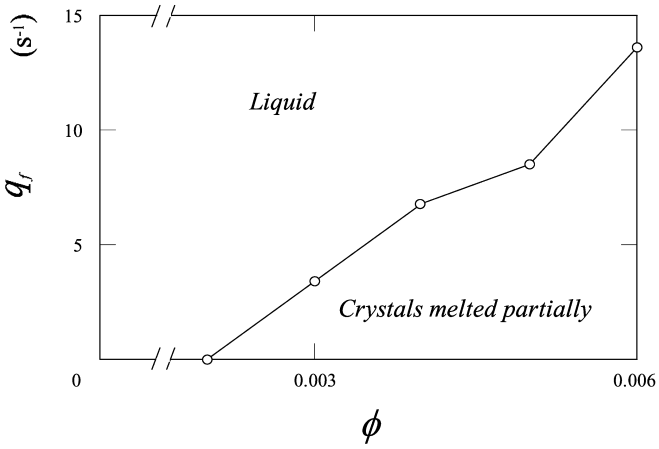

Fig. 8 Relationship between final shear rate (q_f) and volume fraction (ϕ) for the colloidal recrystallization of CS91 spheres at 25 °C. $q_f = 34\ s^{-1}$

Figure 7 shows the time dependence of the reflection peak wavelengths (λ_p) for colloidal crystallization at $q_f = 0\ s^{-1}$, $3.4\ s^{-1}$ and $6.3\ s^{-1}$. Clearly λ_p increased as q_f increased, which supports the idea that the crystals formed in the shear flow are less dense compared to those formed at $q_f = 0$.

Figure 8 shows the relationship between q_f and ϕ for colloidal crystallization. Most crystals coexisted with the melted liquid. Stable crystals were formed only when ϕ was larger than 0.004 and q_f was smaller than $3.4\ s^{-1}$.

Acknowledgements The Frontier Research Project of the Japan Space Utilization Promotion Center is acknowledged for producing the measuring instruments. The Ministry of Education, Culture, Sports, Science and Technology, Japan is thanked for grants-in-aid for Scientific Research in Priority Area (A) (11167241). Drs. M. Komatsu and M. Hirai of Catalyst & Chemical Ind. Co. (Tokyo) are thanked deeply for providing the sample suspension of the colloidal silica spheres.

References

1. Ackerson BJ, Clark NA (1981) Phys Rev Lett 46:123
2. Aastuen DJW, Clark NA, Swindal JC, Muzny CD (1990) Phase Transit 21:139
3. Lowen H, Palberg T, Simon R (1993) Phys Rev Lett 70:1557
4. Grier DG, Murray CA (1994) J Chem Phys 100:9088
5. Wurth M, Schwarz J, Culis F, Leiderer P, Palberg T (1995) Phys Rev E 52:6145
6. Stevens MJ, Falk ML, Robbins MO (1996) J Chem Phys 104:5209
7. Ripoll MS, Tejero CF, Baus M (1996) Physica A 234:311
8. Okubo T (1994) In: Schmitz KS (ed) Macro-ion characterization: from dilute solutions to complex fluids. ACS Symp Series 548. ACS, Washington DC, pp 364–380
9. Okubo T (1994) Langmuir 10:1695
10. Okubo T (1988) J Chem Soc Farad T 1 84:1163
11. Okubo T, Okada S, Tsuchida A (1997) J Colloid Interf Sci 189:337
12. Okubo T, Okada, S (1997) J Colloid Interf Sci 192:490
13. Okubo T, Okada S (1998) J Colloid Interf Sci 204:198
14. Okubo T, Ishiki H (1999) J Colloid Interf Sci 211:151
15. Okubo T, Ishiki H (2000) J Colloid Polym Sci 228:151
16. Okubo T, Tsuchida A, Kato T (1999) Colloid Polym Sci 277:191
17. Okubo T, Tsuchida A, Okuda T, Fujitsuna K, Ishikawa M, Morita T, Tada T (1999) Colloid Surface A 160:311; (1999) Colloid Surface A 153:515
18. Okubo T, Tsuchida A, Takahashi S, Taguchi K, Ishikawa M (2000) Colloid Polym Sci 278:202

19. Tsuchida A, Taguchi K, Takyo E, Yoshii H, Kiriyama K, Okubo T, Ishikawa M (2000) Colloid Polym Sci 278:872
20. Okubo T, Ishiki H, Kimura H, Chiyoda M, Yoshinaga K (2002) Colloid Polym Sci 280:290
21. Yoshinaga K, Chiyoda M, Ishiki H, Okubo T (2002) Colloid Surface 204:285
22. Pusey PN, van Megen W (1987) In: Safan SA, Clark NA (eds) Complex and supramolecular fluids. Wiley, New York, pp 673–698
23. Davis KE, Russel WB (1988) Ceram Trans B 1:693
24. Russel WB (1990) Phase Transit 21:127
25. Harkless CR, Singh MA, Nagler SE, Stephenson GB, Jordan-Sweet JL (1990) Phys Rev Lett 64:2285
26. Dhont JKG, Smits C, Lekkerkerker HNW (1992) J Colloid Interf Sci 152:386
27. Schatzel K, Ackerson BJ (1992) Phys Rev Lett 68:337
28. Schatzel K, Ackerson BJ (1993) Phys Rev E 48:3766
29. Verhaegh NAM, van Blaaderen A (1994) Langmuir 10:1427
30. Butler S, Harrowell P (1995) Phys Rev E 52:6424
31. van Megen W (1995) Transport Theor Stat 24:1017
32. Ackerson BJ, Schatzel K (1995) Phys Rev E 52:6448
33. Rintoul MD, Torquato S (1996) J Chem Phys 105:9258
34. He Y, Ackerson BJ, van Megen W, Underwood WM, Schatzel K (1996) Phys Rev E 54:5286
35. Harland JL, van Megen W (1997) Phys Rev E 55:3054
36. Derber S, Palberg T, Schatzel K, Vogel J (1997) Physica A 235:204
37. Phan SE, Li M, Russel WB, Zhu J, Chaikin PM, Lant CT (1999) Phys Rev E 60:1985
38. Amos RM, Parity JG, Tapster PR, Shephend TJ, Kitson SC (2000) Phys Rev E 61:2929
39. Heymann A, Sinn C, Palberg T (2000) Phys Rev E 62:813
40. Jardine RS, Barglett P (2002) Colloid Surf 211:127
41. Vanderhoff W, van de Hul Hj, Tausk RJM, Overbeek JTG (1970) In: Goldfinger G (ed) Clean surfaces: their preparation and characterization for interfacial studies. Marcel Dekker, New York, pp 13–44
42. Hiltner PA, Papir YS, Krieger IM (1971) J Phys Chem 75:1881
43. Kose A, Ozaki M, Takano K, Kobayashi Y, Hachisu S (1973) J Colloid Interf Sci 44:330
44. Williams R, Crandall RS, Wojtowicz PJ (1976) Phys Rev Lett 37:348
45. Mitaku S, Ohtsuki T, Enari K, Kishimoto A, Okano K (1978) Jpn J Appl Phys 17:305
46. Lindsay HM, Chaikin PM (1982) J Chem Phys 76:3774
47. Peranski P (1983) Contemp Phys 24:25
48. Ottewill RH (1983) Ber Bunsen Phys Chem 89:517
49. Aastuen DJW, Clark NA, Cotter LK, Ackerson BJ (1986) Phys Rev Lett 57:1733
50. Pusey PN, van Megen W (1986) Nature 320:340
51. Okubo T (1988) Acc Chem Res 21:281
52. Russel WB, Saville DA, Schowalter WR (1989) Colloidal dispersions. Cambridge Univ Press, Cambridge, UK
53. Stevens MJ, Falk ML, Robins MO (1996) J Chem Phys 104:5209
54. Okubo T (1993) Prog Polym Sci 15:481
55. Okubo T (1997) Curr Top Colloid Interface Sci 1:169
56. Okubo T (2001) In: Hubbard A (ed) Encyclopedia of surface and colloid science. ACS, Washington DC
57. Wilson HA (1900) Philos Mag 50:238
58. Frenkel J (1932) Phys Z Sowjetunion 1:498